Examining biofilm growth and metabolism of Escherichia coli at laboratory scale using geoelectrical methods

Martin, Tina; Paul, Catherine J. ; Åkesson, Sofia

Published in:
Vatten: tidskrift för vattenvård /Journal of Water Management and research

2023

Document Version:
Publisher's PDF, also known as Version of record

EXAMINING BIOFILM GROWTH AND METABOLISM OF ESCHERICHIA COLI AT LABORATORY SCALE USING GEOELECTRICAL METHODS

GEOELEKTRISKA UNDERSÖKNING AV BIOFILM-TILLVÄXT OCH METABOLISM HOS *ESCHERICHIA COLI* I LABORATORIESKALA



Tina Martin[1], Sofia Åkesson[2] and Catherine J. Paul[3,4]

[1] *Lund University, Faculty of Engineering, Department of Biomedical Sciences, Division of Engineering Geology, Lund, Sweden*
[2] *Lund University, Department of Geology, Lund, Sweden*
[3] *Lund University, Faculty of Engineering, Division of Water Resources Engineering, Department of Building and Environmental Technology, Lund, Sweden*
[4] *Lund University, Faculty of Engineering, Division of Applied Microbiology, Department of Chemistry, Lund, Sweden*
Corresponding author: Tina Martin (tina.martin@tg.lth.se)

Abstract

To link geophysical field data to specific biological phenomena, controlled laboratory experiments are needed for the understanding of the response of geophysical parameters to changes in biological conditions. In this study, suspensions of bacteria were mixed with sand to create a biofilm growing on a surface and these mixtures were monitored using the geoelectrical spectral induced polarization method (SIP). The beginning growth of the biofilm was confirmed by scanning electron microscopy and the amount of bacteria in liquid and sand estimated using culture and DNA based methods (i.e. qPCR, quantitative polymerase chain reaction). While changes in SIP signal could not be clearly related to microbial activity, fluctuations in the phase shift were concomitant with the detection of two unidentified metabolites in the liquid extracted from the sand. These metabolites were only detected when the biofilm was produced under oxygen limiting conditions. Even though the experimental design was not optimal for the SIP measurements, the results support the idea that these measurements are not measuring cell mass but are influenced by the presence of smaller charged molecules that may be produced as microbial metabolites. As microbial metabolites would change in the field during bioremediation, this method could be applied for this type of monitoring.

Sammanfattning

För att relatera geofysiska fältdata till specifika biologiska fenomen krävs en djupare förståelse. I denna studie har 30 kontrollerade laboratorieexperiment genomförts för att därigenom öka kunskapen om geofysiska parametrars respons på förändringar av biologiska förhållanden. Bakteriesuspensioner har blandats med sand för att skapa en biofilm som växer på ytor, för att därefter övervakas med den geoelektriska metoden spektral inducerad polarisation (SIP).Tillväxt av biofilm bekräftades genom svepelektronmikro-

skopi och mängden bakterier i vätska och sand undersöktes med både odlings- och DNA-baserade metoder (t.ex. qPCR kvantitativ polymeraskedjereaktion). Det var inte möjligt att tydligt relatera förändringar i SIP-signalen till mikrobiell tillväxt, men fluktuationer i förskjutning skedde samtidigt som detektering av två oidentifierade metaboliter i vätskan. Dessa metaboliter upptäcktes endast när biofilmen producerades under syrebegränsande förhållanden. Den experimentella designen var inte optimal för SIP-mätningarna men trots detta stödjer resultaten idéen att mätningarna inte påverkas av cellmassan utan närvaron mindre laddade molekyler som produceras som mikrobiella metaboliter. Då mikrobiella metaboliter förändras i fält under bioremediering skulle denna metod kunna användas för övervakning av saneringar.

Keywords: Biofilm, Geophysics, SIP, Bacteria, Metabolites, SEM, qPCR, HPLC

Introduction

Contaminated sites are common around the globe and have been associated with negative effects on human health and the environment (e.g., Rodrigues & Römkens, 2018). In Europe, there are an estimated 2.8 million potentially contaminated sites; however, only 24% have been inventoried (EEA, 2019). Often, contaminated sites contain unconsolidated sediment and flowing water, and can be a risk to drinking water supplies (Burri et al., 2019). There are several possible methods that can be used to remove subsurface contamination, depending on the contaminant and the geological setting. One possible approach is bioremediation at the site of the contamination, via biodegradation. This approach can be due to natural microbes, or these processes can be enhanced, by stimulating the natural occurring biota or by addition of microbes (Stroo et al., 2013). One gram of soil can contain more than a billion microbial cells which can span an enormous number of different species and their diverse metabolisms, that in some cases are able to remove complex molecules (Voroney, 2007). However, since often both the microbes and contamination are located deep in the subsurface, it is difficult to follow the progress of bioremediation in situ while the biological reactions are occurring to remove the contamination. Improved methods for monitoring in situ bioremediation would also facilitate evaluations of the effectiveness of any interventions.

Geophysical measurements have been applied to investigate a range of contaminated sites (Atekwana et al., 2004b; Cardarelli & Di Filippo, 2009; Flores Orozco et al., 2012; Power et al., 2014; Johansson et al., 2015; Sparrenbom et al., 2017; Nivorlis et al., 2019; Åkesson et al., 2020) and it would be beneficial if these could also be applied to monitor degradation processes, as the disturbance during these investigations is lower than with more conventional methods. Spectral induced polarization (SIP) method has shown promise for detection and monitoring bacterial activities in the subsurface (Atekwana & Slater, 2009; Atekwana & Atekwana, 2010; Kessouri et al., 2019). SIP could contribute to the characterization of contaminated sites and bioremediation processes and can be applied to measure biomineralization, cell properties and biofilm (Atekwana et al., 2004b; Flores Orozco et al., 2011; Flores Orozco et al., 2012). Studies have proposed that bacterial cells directly influence the SIP signal as the cells can be polarized and negatively charged due to the presence of a polymeric brush layer which allows the development of an electrical double layer (Atekwana & Slater, 2009; Kessouri et al., 2019). Indirectly, bacteria also contribute to changes in the chemistry of the material and fluids in the ground, and hence change electrical properties, in either the fluid (Prodan et al., 2004) or by weathering and dissolution of minerals and surfaces (Atekwana et al., 2004a).

In natural settings, bacteria often grow as biofilm (Branda et al., 2005). Biofilm is formed by one or more types of bacteria on a surface, such

as a sand grain. It is thought that biofilm is polarizable as it is a matrix comprised of bacterial cells, but also extracellular polymeric substances, DNA, fluids and non-cellular material such as dissolved nutrients (Rosier et al., 2019; Kessouri et al., 2019) and thus changes in the arrangements or surface properties of the cells, or changes in the production of extracellular substances or charged nutrient species could be detected by SIP. Growth or detachment of biofilm in response to changes in the environment could also change flow paths for liquids or current by causing clogging of pores (Brovelli et al., 2009). Gas migration has been monitored with IP (induced polarization) and, as gaseous molecules can also be a metabolite of bacterial degradation processes, this could also affect the biofilm and lead to additional changes in pore clogging and flow (Rosqvist et al., 2011; Auken et al., 2014). The investigation of biofilm growth and response to the SIP signal has been investigated (e.g., Davis et al., 2006, 2010; Albrecht et al., 2011), however, most of the previous studies have used a flow-through approach with measuring in a column (e.g., Ntarlagiannis et al., 2005; Saneiyan et al., 2018).

In the present study, growth of biofilm took place outside the column and was measured in a static condition that was thought to be closer to the natural conditions in slow or with nonexistent temporal changes, e.g., groundwater flow. Controlled laboratory experiments were designed to observe how IP changed over time, and how this correlated to growth or other properties of *Escherichia coli* (*E. coli*) growing in a biofilm. Mixtures of sand and bacteria were incubated in different ways and SIP measurements were compared to the amount of *E. coli* (henceforth also referred to as "bacteria") present both as suspended cells in liquid and growing as biofilm on the surface of the sand. That cells were present as biofilm was described using scanning electron microscopy and the bacterial cell numbers in the biofilm were quantified using quantitative polymerase chain reaction (qPCR). Charged metabolites produced by the bacteria in the biofilm that may have been influencing SIP signals were considered as well, and identity, presence, and quantity were measured using high performance liquid chromatography of pore liquid extracted from the sand-biofilm mixtures.

By examining specific controlled responses in SIP from a biofilm grown under highly defined conditions, this study sought to improve the understanding of SIP responses that could be associated with microbial processes in the nature, such as metabolic activity during bioremediation. The study is part of the research project MIRACHL (www.mirachl.com), which seeks to monitor remediation actions using geoelectrical methods in combination with information about changes in chemical concentrations and microbial properties.

Material & Methods

2.1 Spectral induced polarization method

Induced polarization (IP) measures the temporary, reversible storage of charge (polarization process) in addition to the electromigration of the charge by conduction (Binley & Slater 2020). IP can be measured in time-domain by applying a current and measuring the voltage drop after switching off the current, or by measuring in the frequency-domain by applying sinus waves with different frequencies. This study uses the frequency-domain method in a broad frequency range. This method is referred to as spectral induced polarization (SIP). The SIP survey is performed by an impedance spectrometer that registers the amplitude of impedance and the phase shift between injected sinusoidal current signal and measured voltage. The resulting impedance Z is a complex frequency dependent quantity

$$Z(\omega)=|Z(\omega)|ei^{\phi(\omega)}, \quad (1)$$

with $\omega=2\pi f$ being the angular frequency, $i=\sqrt{(-1)}$ the imaginary unit, and $\phi(\omega)$ the spectrum of the phase shift. The multiplication of the complex impedance by a geometric factor k yields a complex, frequency-dependent resistivity $\rho^*(\omega)$ and is often presented in resistivity magnitude $|\rho|$ and phase ϕ:

$$\rho^* = |\rho| e^{i\phi} = \rho'+i\rho'' \quad (2)$$

With ρ' as real and ρ" as imaginary part of resistivity and i=√(-1) as imaginary unit. Instead of resistivity, data can also be presented as conductivity value $\sigma^* = 1/\rho^*$.

Here, σ' describes the electrical conduction within a material whereas σ" describes the polarization part and can be calculated as

$$\sigma' = |\sigma| \cos \phi \quad (3) \quad \text{and} \quad \sigma'' = |\sigma| \sin \phi \quad (4)$$

In a material, two electrical current transfers can occur (assuming non-metallic minerals): the electrolytic conduction (σ_{elec}), which takes place through connected pores, and the surface conduction (σ_{surf}) which takes place in the electric double layer at the mineral-fluid-interface (or in our case at the bacteria-fluid interface). By assuming parallel conduction paths (Waxman & Smits, 1968) the electrolytic and surface conduction is connected as:

$$\sigma' = \sigma'_{elec} + \sigma'_{surf} \quad (5) \quad \text{and} \quad \sigma'' = \sigma''_{surf} \quad (6)$$

It is thus possible to discriminate both conduction paths which makes the method very sensitive to any changes in the surface/pore space structure and potentially detect changes caused by bacteria and biofilm.

2.2 SIP measurements

The SIP response was measured by the PSIP instrument (Ontash & Ermac, 2018) applying sine wave in the frequency between 1 mHz and 20 kHz. The impedance Z and the phase ϕ are calculated based on the induced voltage (V) and the stimulus current (I). Based on a "current sense resistor" within the instrument and the value of this resistor (R), the stimulus current (I) is computed using the Ohm's law (I = V/R, see Ontash & Ermac, 2018). The bacteria-sand mixtures were placed in a cylindrical 4-point sample holder as described in Kruschwitz (2008). It includes stainless steel plate electrodes for the current injection and silver-wire ring electrodes for the potential measurements. The sample holder was tested with tap water before the bacteria experiments started. The accuracy of the sample holder and the instrument was 2% for the resistivity and < 0.2 mrad for frequencies < 100 Hz. The sand mixtures were packed stepwise into the holder with a constant pressing after removing suspension liquid by filtering. The resulting density for all samples was between 2.74 and 3.05 g/cm^3. The conductivity of the fluid was measured with a conductivity meter from the company WTW (https://www.wtw.com/en/). The laboratory environment generated interference in some data at a frequency of 50 Hz.

Table 1: *Experimental design for all test series.*

Test	Description	Number of samples	Harvest at day	Shaker (rpm)	Samples Ingredients
WS	Water-sand samples	8	1, 2, 3, 6, 9, 13, 16, 21	80	150 ml milli-Q water + 0.75 g NaCl + 240 g Ottawa sand
MS	Media-sand samples	8	1, 2, 3, 6, 9, 13, 16, 63	80	150 ml Media + 240 g Ottawa sand
ES-1	*E. coli* - sand samples, single concentration	8	1, 2, 3, 6, 9, 13, 16, 21	80	*E. coli* (0.15 ml) + 150 ml Media + 240 g Ottawa sand
ES-2	*E. coli* - sand samples, single concentration	9	0, 1, 2, 3, 4, 5, 6, 7, 8	80	*E. coli* (0.15 ml) + 150 ml Media + 240 g Ottawa sand
ES-doub	*E. coli* - sand samples, double concentration	9	0, 1, 2, 3, 4, 5, 6, 7, 8	160	*E. coli* (0.3 ml) + 150 ml Media + 240 g Ottawa sand

2.3 Growth of bacteria-sand mixtures

Sterile 500 mL flasks were inoculated with 150 mL liquid (either sterile MilliQ water, or Luria Bertani (LB) media, depending on the experiment), bacterial inoculum if using, and 240 g sterile new Ottawa sand. The growth media LB was prepared with 10g tryptone, 5g NaCl, 5g yeast extract per litre. Ottawa sand is very homogeneous and well described (Erdoğan et al., 2017) with a particle size of 0.6 – 0.8 mm. The sand was not re-used. Flasks were inoculated with either 150 or 300 µL (depending on the experimental setup, see Table 1) of an overnight culture of *E. coli* strain DSM1116, when used. This is a safe and easily grown variant of *E. coli*, that, in contrast to other widely used *E. coli* laboratory strains, remains free of genetic modifications and was isolated from a natural source (Archer et al., 2011). The bacteria-sand mixtures were incubated with shaking at either 80 or 160 rpm (rotations per minute) at 30°C until the mixtures and liquid were harvest for analysis (Figure 1a). After each SIP measurements parts of the samples were kept for the subsequent investigations. The rest of the samples was discarded.

2.4 Quantitative polymerase chain reaction (qPCR) measurements

The number of *E. coli* (DSM1116) growing in the sand was determined using qPCR (quantitative Polymerase Chain Reaction). This determines the number of copies of a specific gene in a defined starting mass and with a select target profile (Berg et al., 2006). In this study the 16S rRNA gene was the target gene, with specificity to detect all bacteria (Nadkarni et al., 2002). Template DNA was extracted from approximately 0.5 g of sand-mixture, selected from days 2, 6, 13, and 16, using the FastDNA™ Spin Kit for soil, following manufacturer's instructions. qPCR was conducted using primers, probe and thermocycling conditions as previously described (Nadkarni et al., 2002). A reaction volume of 20 µL contained 5 µL of template DNA, 1X ExTaq Buffer (TaKaRa), 0.2 mM dNTPs, 2 mM MgCl2, 0.3 µM of each primer, 0.2 µM TaqMan DNA probe, 0.1 mg/mL bovine serum albumin (BSA), and 0.05 U/µL ExTaq HS. The qPCR was run in a thermal cycler (Roche LightCycler 2.0) in high quality mode, with an initial denaturation for 15 min at 95°C followed by 45 cycles of: denaturation at 95°C for 10 s, annealing at 60°C for 20 s and elongation at 72°C for 30 s. All samples were run in duplicates. Chromosomal DNA from *E. coli* DSM1116 was used as the control in a standard dilution series that had been quantitated with ThermoFisher Qubit Florescence 3.0.

2.5 Scanning electron microscope

A scanning electron microscope (SEM) was used to confirm any presence of bacteria attached to the sand and to visualise bacteria growing. Sand grain samples were washed twice in 0.1M Sorensen´s phosphate buffer pH 7.4 to remove media and then fixed in approximately 10 times the sample volume of "SEM fix" (0.1M Sorensen´s phosphate buffer pH 7.4, 2% formaldehyde and 2% glutaraldehyde) at room temperature for 15-20 minutes. After fixation, samples were washed twice in 0.1M Sorensen´s buffer pH 7.4 to remove excess fixative. Samples were dehydrated in a graded series of ethanol (50%, 70%, 80%, 90% and twice in 100%), critical point dried and mounted on 12.5 mm aluminium stubs and subsequently sputtered with 10nm Pt/Pd (80/20) in a Quorum Q150T ES turbo pumped sputter coater and examined in a Jeol JSM-7800F FEG- SEM.

2.6 Plate counting

The concentration of live bacteria in the fluid of the samples was determined by plating a dilution series of the collected fluid (water or LB media) on LB agar (LB media, see above, 1.5% agar) after Elbing & Brent (2019). Colonies were counted by visual inspection following incubation of plates for 24 h at 37°C.

2.7 High performance liquid chromatography (HPLC)

From each of the wet sand samples, liquid was extracted to assess the presence of any metabolic products released from the biofilm. For each sample, 10 g of sand was loaded into cell strain-

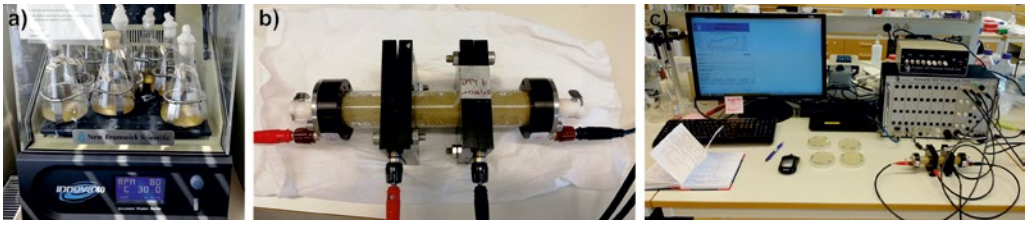

Figure 1: *Experimental design. a) The samples were kept in the shaker until harvest (30°C and 80/160 rpm); b) SIP sample holder filled with saturated bacteria-sand mixtures; c) used SIP Instrument incl. 4 plate counting samples (in the middle).*

ers (Falcon, cut-off 45 µm) and saturating liquid was separated from sand using a 3-minute centrifugation at 3000 rpm in a swing bucket rotar. This liquid was then centrifuged a second time at 13 000 x g for 5 minutes to remove any bacterial cells or other debris. The supernatant was removed and water-soluble metabolite products (such as acetate, glucose) in this liquid were determined by high-pressure liquid chromatography with a RI-detector (RID-6A, Shimadzu, Kyoto, Kyoto prefecture, Japan). Metabolites were separated on two Rezex ROA-Organic Acid H+ (8%) ion exclusion columns (00F-0138-E0, Phenomenex, Torrance, CA, USA) in series, with 5 mM H2SO4 as the mobile phase (0.6 mL/min) at room temperature (22°C).

2.8 Experimental design

To investigate the influence of the bacteria and any biofilm formation in a sandy environment on the SIP signal, the following tests were conducted:

- Water - sand mixture (WS) which acts as a reference test series.
- Media - sand mixture (MS) to get information about the influence only from the media.
- First *E. coli* – sand mixture (ES-1) to get information about the influence of the bacteria.
- Second *E. coli* – sand mixture (ES-2) to verify the first tests and to focus on the first 8 days.
- *E. coli* – sand mixture (ES-doub) with the double initial amount of bacteria and higher shaker velocity to get information about the influence of the concentration and the expected higher velocity stress on the bacteria and biofilm formation.

Media is used here as the term to describe the nutrient solution which supports microbial growth. After running the WS, MS and ES-1 experiments for up to 21 days, the first eight days were then used for the ES-2 and ES-doub samples since it was during this period that most of the changes were observed. Note, the first measurement for the samples WS, MS, ES-1 were performed after 24 h (Day 1) while for the ES-2 and ES-doub samples an additional measurement was performed directly after the mixing (Day 0). The detailed parameters for the experimental design can be found in Table 1.

The experiment workflow is described as (see also Figure 2): On selected days, one flask from each mixture was taken, and the fluids part were filtered from the sand. The fully saturated sand was then packed into the SIP sample holder and measured (Figure 1b and c). Bacteria in the filtered fluid were counted and the same fluid was used for conductivity measurements. The sand was stored at -20°C until DNA extraction for qPCR, extraction of metabolites and SEM was carried out.

3 Results

3.1 SIP measurements and fluid conductivity

The conductivity of the filtered fluid σw was measured on all days when the sand was harvested (Figure 3). The conductivity was very high for all samples (approx. 1 – 1.5 S/m) due to the high-salinity of the media resp. the water. The water controls without bacteria and media (WS) showed the lowest conductivities (around 1 S/m), followed by the media-sand mixtures (MS). For both test series, an increase in conductivities over time can be seen that is not related to microbial activity. All three

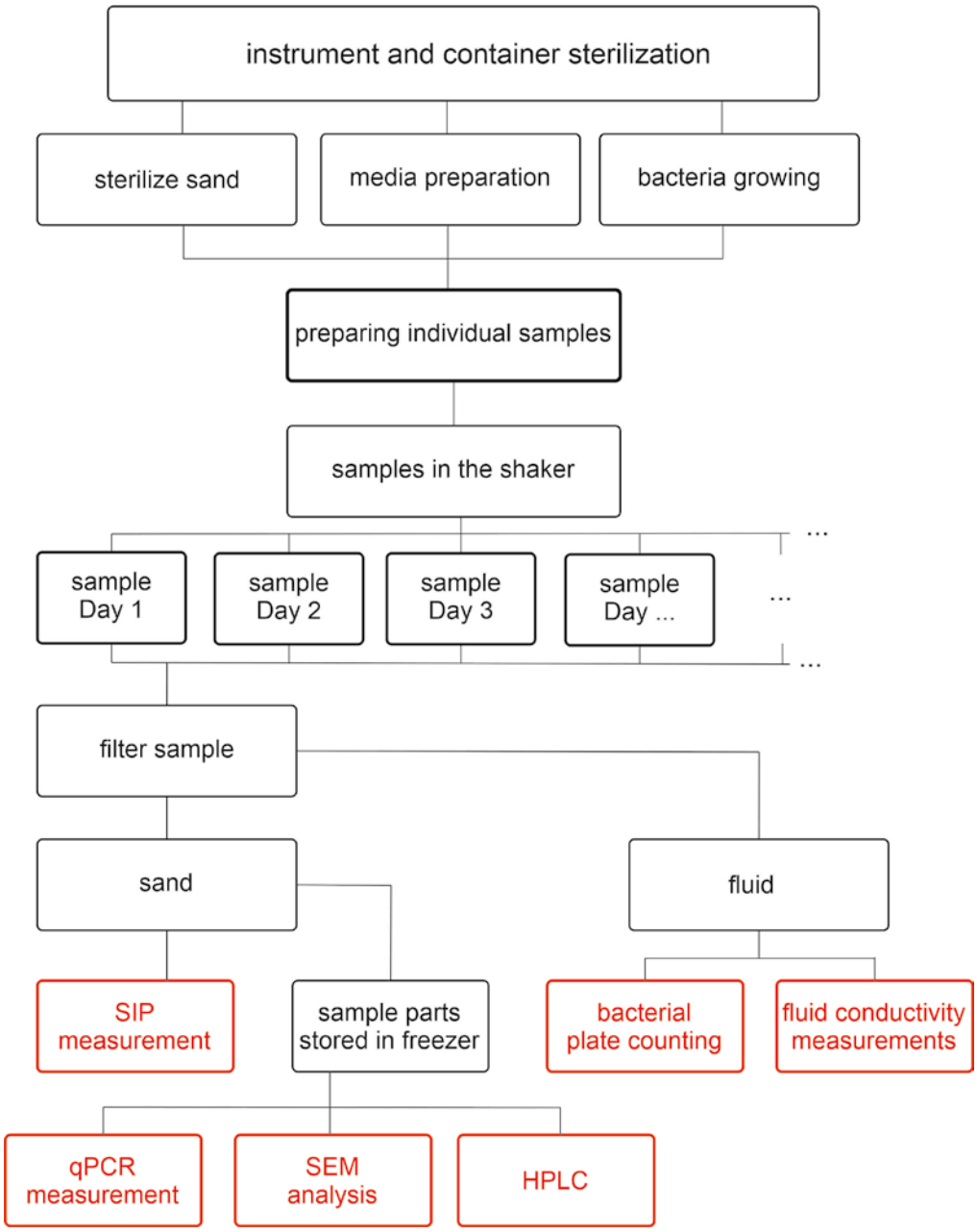

Figure 2: *Workflow of the bacteria measurements.*

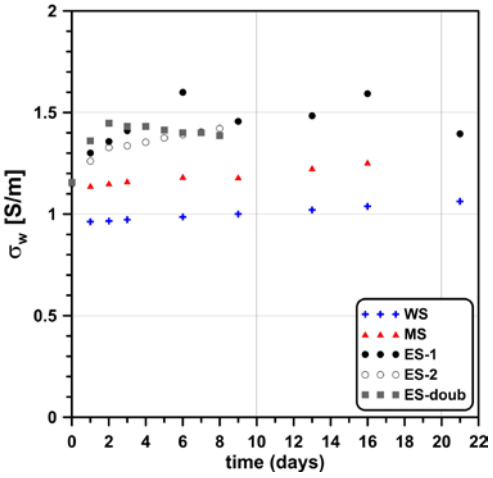

Figure 3: *Fluid conductivity from the filtered fluid for all mixtures at specific time dates ("harvest time").*

sample series with the bacteria showed the highest conductivities (> 1.3 S/m) although they differed in their behaviour. The ES-2 samples showed an increase of conductivity over the entire time. ES-1 samples showed an increase until Day 6, and then became quite variable. The ES-doub samples reached a maximum in conductivity at Day 2 and decreased slightly thereafter.

At specific time dates ("harvest time"), the SIP response for all sand-sample mixtures was measured. The results for the first test series are shown in Figure 4 in terms of resistivity (a, c, e) and phase (b, d, f) in the frequency range between 10 mHz and 1 kHz. Due to some noisy phase data for the ES-1 samples from Day 1 and Day 3, these samples were not included in Figure 4f.

Most of the water-sand (a) samples showed constant resistivities around 5 Ωm across the frequency range. Only the samples from Day 9 and 16 showed higher values (7.5 Ωm resp. 8.5 Ωm). In phase (b), the changes across the frequencies were small (+/- 0.4 mrad) with no clear maximum or minimum. The media-sand samples (c, d) showed a similar behaviour with very small constant phase effects (+/- 0.4 mrad). Only the sample on Day 16 showed slightly pronounced maxima. In resistivity (c), the variation was higher. Even though most of the samples showed resistivities around 5 Ωm, there were some samples with higher values (MS-Day 6: 8.3 Ωm; MS-Day 16: 9.2 Ωm; MS-Day 13: 12.2 Ωm). A significant change in resistivity (Figure 4e) could be observed for the samples with the bacteria (ES-1). Although two samples had differing resistivities (Day 2 and 21), most showed values around 4 Ωm. More variation was seen in the phase shift (f), even though the values were still small (max. 2 mrad). Here, clear changes were visible for the Day 6 sample which showed the highest (positive) phase effect (1.7 mrad) at 6 Hz. At a similar frequency, Day 21 sample had a phase maximum (approx. 0.6 mrad). The rest of the samples showed variation within +/- 0.4 mrad.

As Day 6 had the highest phase effect for the ES-1 samples (Figure 4f), the direct comparison of the results from the bacteria – sand mixtures (ES-1) with the reference mixtures (WS and MS) for that date are shown in Figure 5.

In accordance with the fluid conductivity σw (Figure 3), the ES-1 sample showed the lowest resistivity values (a) in comparison with the MS and WS samples. In contrast to the expected higher resistivity of the WS sample, it was the MS sample which showed the highest resistivity. Usually, most of the MS samples showed resistivities around 5 Ωm (Figure 4c). Higher values were observed for some outliers, and one of them is MS Day 6. The reason for these deviations is still not clear but one explanation might be packing effects (air closure). In phase (b), a clear distinction between the samples with the bacteria and the reference samples (WS, MS) was observed. Whereas the reference samples gave phase values between +/- 0.2 mrad, the ES-1 sample showed much higher values.

The SIP spectra for the second test series with only samples containing *E. coli* (ES-2 and ES-doub) (Figure 6) showed that, even though the test serie ES-2 was a repetition of the first 8 days of the series ES-1, the results differed. In Figure 6a the variability in resistivity was large and varied between 3 and 13 Ωm. The phase signals (b) were in a range between +/- 0.5 245 mrad without showing a significant phase maximum at any time. For the samples with the double initial amount of bacteria (ES-doub) the resistivity range was very nar-

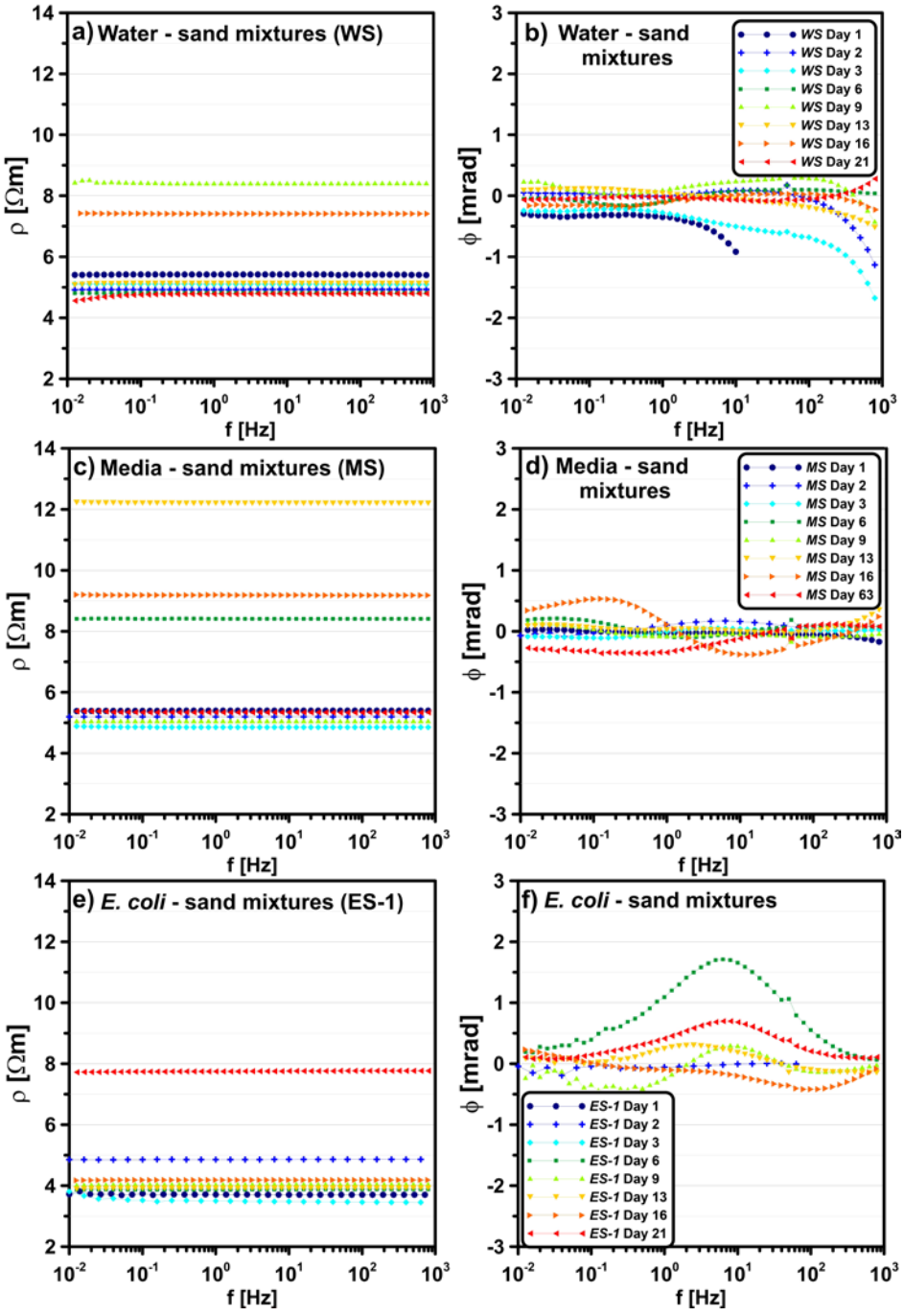

Figure 4: *SIP results for the water-sand (WS, a, b), media-sand (MS, c, d) and bacteria – sand mixtures (ES-1, e, f) at different days of harvest; a, c, e) resistivity, b, d, f) phase. Due to some noisy phase data for ES-1 samples at Day 1 and Day 3, these samples are not included in Figure 4f. Note: At the frequency of 50 Hz, interference from the laboratory environment occurred occasionally.*

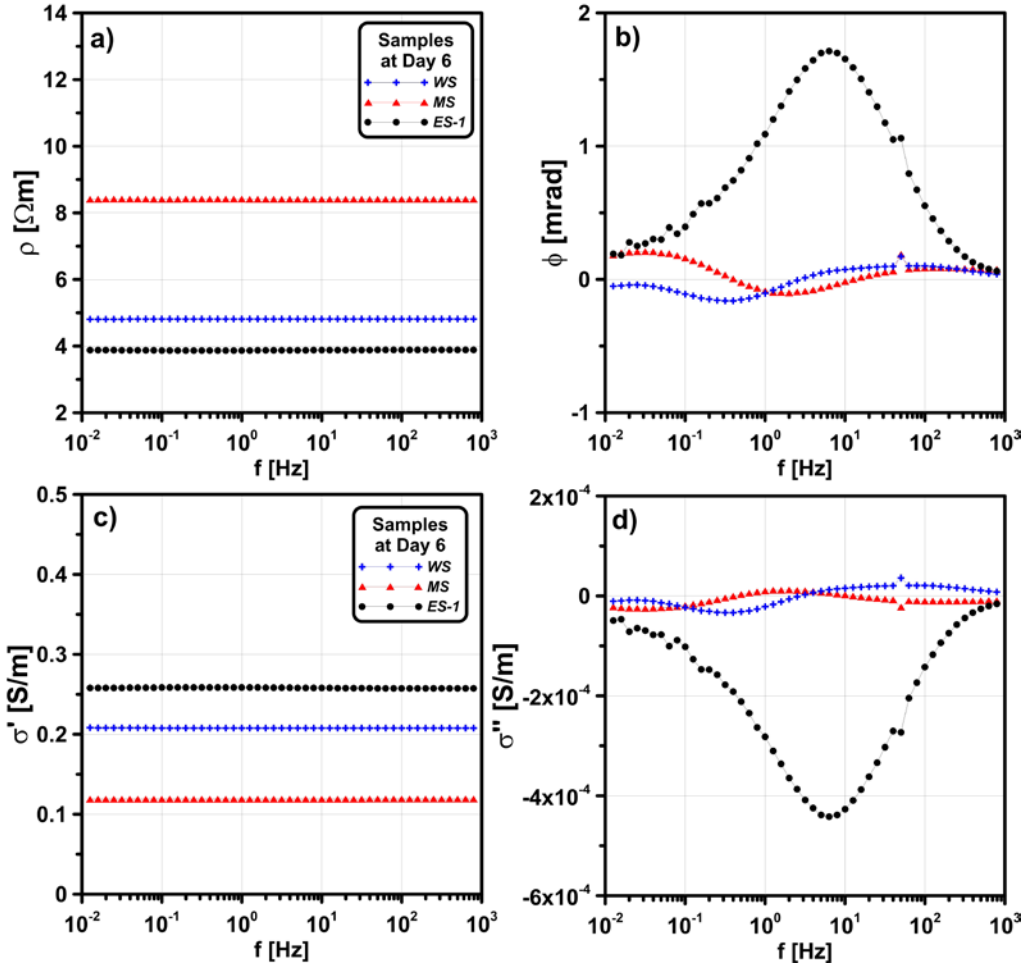

Figure 5: *SIP spectra for Day 6 for the water – sand (WS), media – sand (MS) and bacteria – sand (ES-1) samples. a) resistivity, b) phase. Note: At the frequency of 50 Hz, interference from the laboratory environment occurred occasionally.*

row and lay between 4.2 and 6.2 Ωm (Figure 6c). Despite the higher number of bacteria, in phase (d), the signals were still very small and in a range between +/- 1 mrad. Two of the samples showed a maximum phase peak in the medium frequency range (Day 3 and 5).

The results at 1 Hz in terms of resistivity (a), phase shift (b), real (c) and imaginary conductivity (d) were compared (Figure 7). At first glance, the data did not show any clear trend with time although some tendencies could be observed. Variation in resistivity (a) and real conductivity (c) for the control samples that did not contain bacteria (red and blue) appears slightly higher than for those with *E. coli*. In phase (b) and imaginary conductivity (d) the opposite was observed. Most of the changes in phase resp. imaginary conductivity were seen for the ES-1 samples and less changes were associated with the media-sand samples.

3.2 Quantifying the bacteria in liquid and sand

In order to understand the possible relationship between signals obtained from the SIP measurements and biological changes, bacteria were quantitated

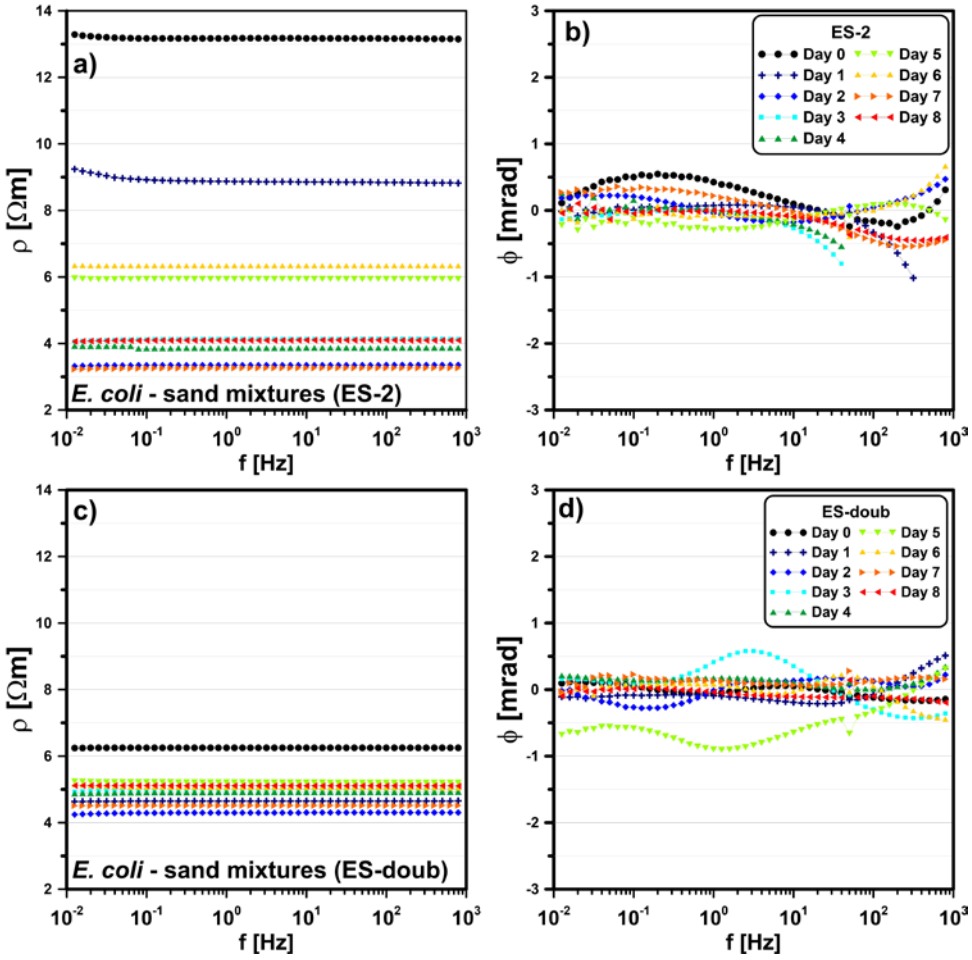

Figure 6: *SIP results for the second test serie, only containing bacteria – sand mixtures (ES-2, ES-doub) at different days of harvest; a, c) resistivity, b, d) phase. Note: At the frequency of 50 Hz, interference from the laboratory environment occurred occasionally.*

in both the liquid and sand from the different experiments (Figure 8). Plate counts reflect live bacteria in the liquid phase, reported as colony forming units per millilitre (cfu/mL), and this peaked two days after the inoculation of the mixtures, reaching up to 6 x109 cfu/mL (Figure 8a). After Day 2, the concentration of live bacteria decreased, likely as nutrients were consumed and cells began to die, although this was different across the three test series. The ES-2 samples had the least die-off, with around 1.0 x 109 cfu/mL present until Day 8. The decrease for the ES-1 samples was much steeper with only 2.0 x 103 cfu/mL after 21 days with an outlier at Day 16. The ES-doub samples showed the steepest decline in live cells with a minimum at 1.0 x 105cfu/mL already reached after 7 days.

No live *E. coli* bacteria could be observed from the plate counting of the water – sand and media – sand samples, as expected.

To get a qualitative number of the bacteria present in sand, qPCR measurements were conducted for a selection of samples from the WS, MS and ES-1 run (Figure 8b). The qPCR measurements have been done DNA extracted from sand removed

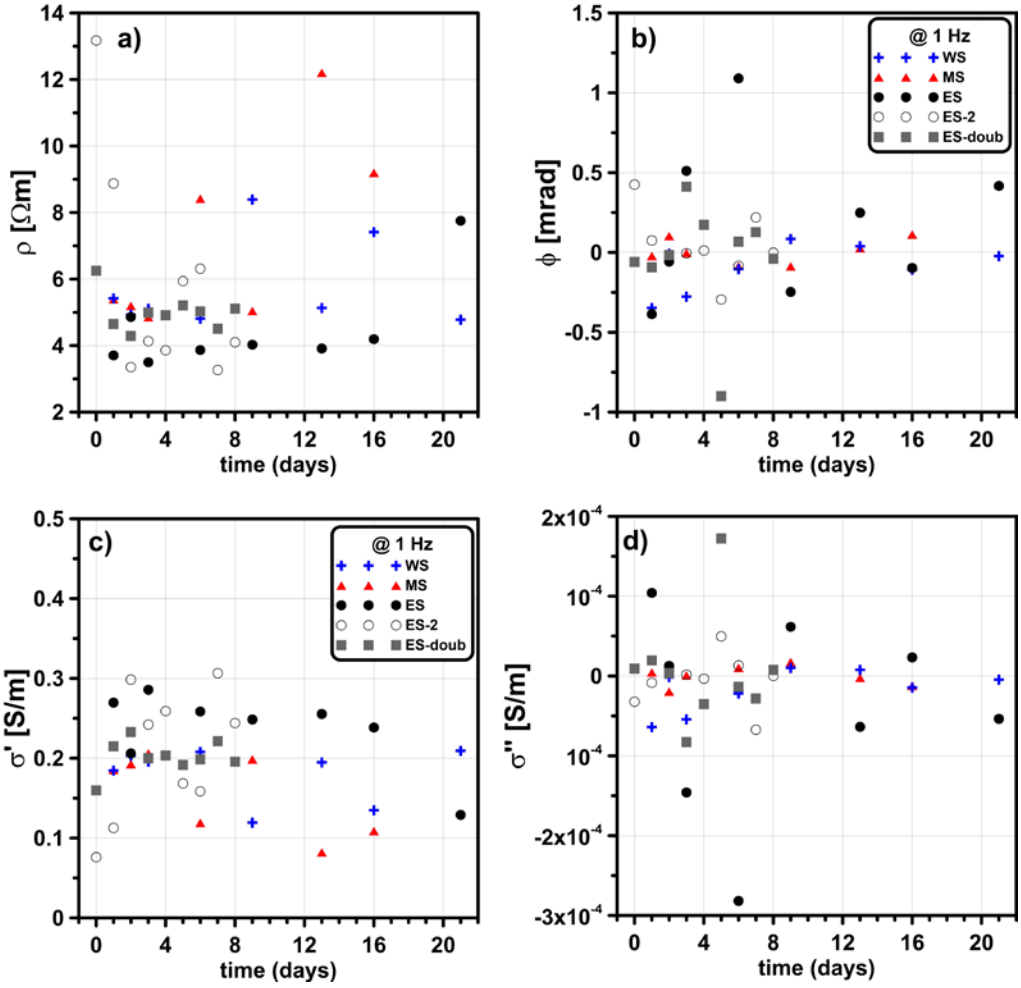

Figure 7: *SIP results for all samples at 1 Hz. a) resistivity, b) phase, c) real conductivity, d) imaginary conductivity.*

from the instrument following SIP measurements using the 16S rRNA gene as the target. This target is not specific for *E. coli* but would also detect any other bacterial growth in the sand that could influence the geophysical measurements. The concentration of 16S rRNA gene copy numbers, which is directly proportional to the amount of any bacteria in the sand, mirrored the changes in bacterial concentration observed in the liquid phase. After Day 2 the number of bacteria in the sand decreased for the bacteria-sand samples. At Day 16 a small increase in bacterial gene copies was observed, which was also observed as an increase in the number of live bacteria in the liquid samples (Figure 8a). No bacterial growth was observed in the water - sand and media - sand mixtures with the exception of the media - sand sample at Day 16 (Figure 8b, circle). This slight increase in bacterial 16S rRNA gene copies for that sample suggests slow growing bacteria present in the sand, which may also explain the different odour observed while harvesting this particular sample. For this sample we could

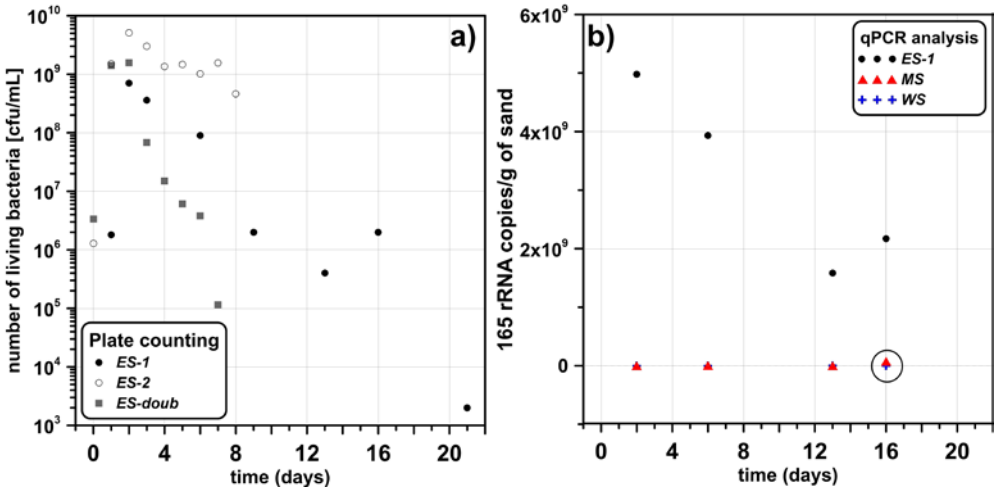

Figure 8: *a) Colony forming units per millilitre (cfu/mL) of E. coli increased after two days, with some differences depending on the specific bacteria – sand mixtures. b) Gene copy numbers for the 16S rRNA gene were calculated per gram of sand, to quantitate all bacterial DNA from bacteria-sand, media-sand and water-sand mixtures for ES-1 only. Bacteria were detected in significant numbers in only those flasks that had been inoculated with E coli. Note: Due to the different experimental design (see Table 1) measurements for ES-1 began on Day 1 whereas those for ES-2 and ES-doub began at Day 0.*

observe a slightly higher negative phase effect than for the rest of the media-sand samples (orange line in Figure 4d). While the sand was sterilized before use, it is possible that spores or other bacteria could have contaminated the sample at some point during the experiments and the long incubation allowed it to grow.

3.3. Visualization of the biofilm

That the sand contained bacteria attached and growing as biofilm was visualized using scanning electron microscopy (SEM). Results (Figure 9) from a representative sample from each mixture (WS/MS/ES-1) showed that bacteria were not attached to the sand in the water - sand (a) and media - sand (b) mixtures, while several areas with bacteria attached to the sand grain could be seen for the bacteria – sand mixtures (c). In panel c, the beginning of biofilm formation was observed (white arrows, "spiderweb" similar structures). Cells are clustered together and strands of exopolysaccaride, the sticky matrix produced by the bacteria to form the biofilm structure, can be observed. An examination of various grains from the bacteria- sand sample also showed uneven colonization by the *E. coli* bacteria, including a preference for grooves and rough edges as expected for biofilm growth (Figure 9c).

3.4 Detection of bacterial metabolites

As the maximum phase shift for the ES-1 Day 6 sample did not coincide with patterns observed by growth, high performance liquid chromatography (HPLC) was performed on pore liquid to assess the presence or absence of metabolites that could explain the observed changes (Figure 10). While some liquid in contact with the biofilm had previously been removed prior to the SIP measurements, additional liquid present in the sand, that had been in close contact with the biofilm, could be extracted from the sand using centrifugation (see section 2.7). Molecules from samples containing sand and media (MS Day 6) were detected as peaks in the chromatogram and identified as glucose, formate, acetate and ethanol by comparison with a standard (Figure 10, panel B). These mole-

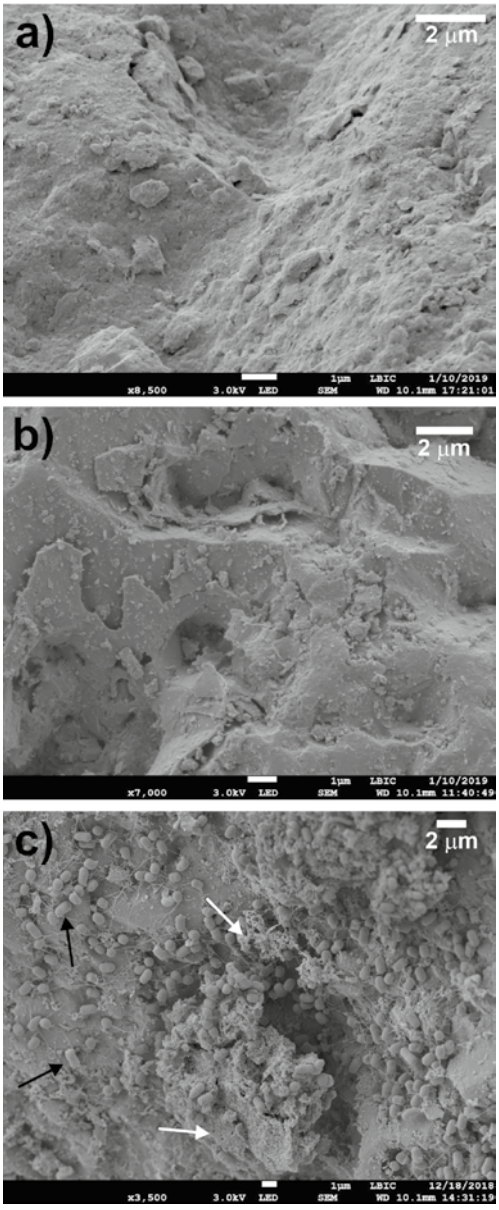

Figure 9: *SEM results for a) water - sand sample, b) media - sand sample, c) bacteria - sand sample (ES-1, Day 6). In c) the individual bacteria cells (black arrows) and the formation of biofilm (white arrows) can be observed.*

cules were not present when only water was used as the liquid in contact with the sand (Figure 10, panel A, WS Day 6), as expected. When bacteria were present in the media (ES-1 Day 6), the peaks identified in the media samples were exchanged for two different peaks (Figure 10, panel C). The retention time of these peaks did not match the retention times of the standards and would require additional analysis for absolute identification. The first unknown had a longer retention time than glucose, but shorter retention time than lactate, and a concentration of 898 g/L. The second unknown had a longer retention time than lactate and a shorter retention time than formate, and a concentration of 2592 g/L. These peaks were not detected from samples at other times points or, when the shaking or the number of bacteria in the samples was increased.

4 Discussion

While the potential for geophysical methods to report on processes linked to bioremediation has been suggested, the complexity of field sites makes it difficult to define the links between the data and specific biological phenomena. One way to address these links is to build up an understanding of the response of geophysical parameters to changes in biological conditions in controlled laboratory experiments. This study used suspensions of bacteria mixed with sand to create a biofilm growing on a surface, with monitoring of the mixtures using SIP. The first signs of creating biofilm could be seen in the SEM results, with additional growth of the biofilm assessed by qPCR targeting all bacteria in the sand. While changes in the SIP signal could not be directly related to bacterial growth, fluctuations in the phase and imaginary conductivity were concomitant with the detection of two unidentified bacterial metabolites in the liquid extracted from the sand.

The bacterial growth of the three bacterial - mixtures showed significant differences (Figure 8a). Whereas a slight bacterial growth decrease for the low concentration mixtures (ES-1, ES-2) can be seen, the decrease for the higher concentration samples is much stronger (ES-doub). One reason for that might be the limited nutrient supply. While adding more initial bacteria for the ES-doub samples, we did not provide any additional nutri-

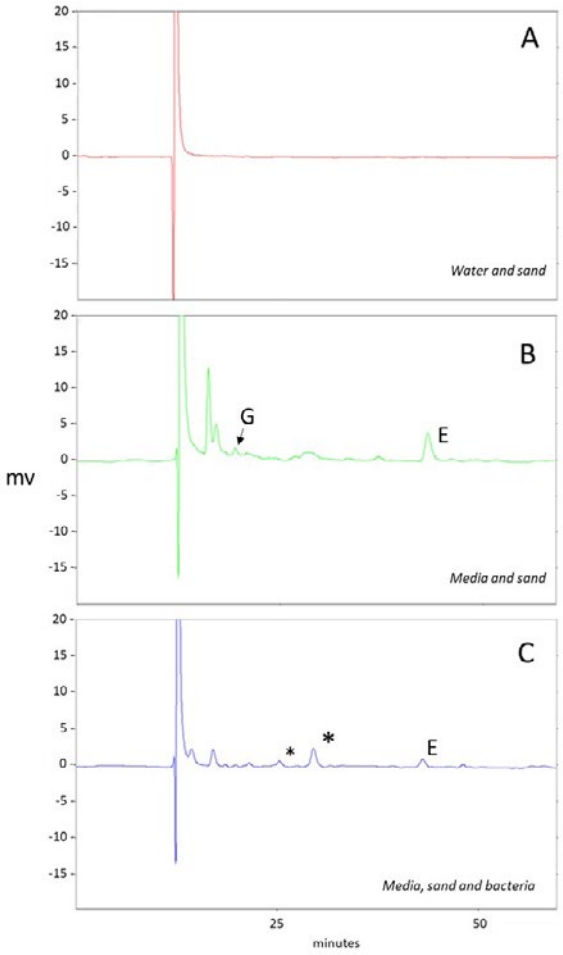

Figure 10: *High performance liquid chromatography traces showing retention time over 50 minutes of different metabolites. Sand pore water was collected from Day 6 samples with reduced shaking and containing: only water and sand (A); media and sand (B); and E. coli in media and sand. This analysis showed two unknown metabolites, where one was in very low amounts (small*) while the other was present at 2592 g/L (large*) in only the pore water extracted from the sand containing E. coli. Due to the age of the instruments, data was available only as screenshots and as the notations on the axes were too small, the labels were added with a graphics software for readability. Original traces are available. "G" indicates peak identified as glucose, "E" indicates peak identified as eth-anol. Large peaks to the right of "G" are likely sucrose and phosphorus but cannot be confirmed as they were not included in the standard.*

ents. Therefore, after two days of microbial growth, the population might have started to starve, and a sudden decrease of living bacteria occurred. An additional explanation can be the toxicity due to the non-removal of microbial by-products, such as volatile compounds (Osborne et al. 2021) and oxidative molecules (Imlay 2013) which can occur under the conditions of the experiment and cause cell death. Comparing the number from the ES-2 samples with the numbers from ES-1, it can be observed that more bacteria were alive within the first 8 days for the ES-2 samples. The only difference between both experiments was the length of the experiment and the time of harvest but this should not have changed the results in the first 8 days. No bacterial contamination was detected in the controls, so the only explanation can be that the inoculation of the bacterial cultures, followed by stochastic effects in the subsequent growth, gave natural fluctuations in the concentrations of bacteria. In future experiments this must be alleviated by including a number of replicates, even though this would be subject to the limiting step of the SIP analysis.

In all experiments within this study, the conductivity of the filtered fluid changed with the mixtures as well as with the time of harvest (Figure 3). The sand mixtures with the bacteria showed higher conductivities than those with media or water alone. That is in accordance with the results from other studies (for example in Prodan et al., 2004) and can be explained by the properties of the electrical double layer of the bacteria (Revil et al., 2012; Kessouri et al., 2019; Mellage et al., 2019). As expected, the sand mixtures with water had the lowest conductivities while the addition of the ingredients for the LB media to support bacterial growth resulted usually in higher conductivities due to components in the yeast extract (soluble peptides, amino acids and trace nutrients) as well as additional tryptone. In the absence of bacteria, the conductivity was slightly increasing with time, and the highest fluid conductivity for the mixtures containing bacteria was reached after 6 days for the ES-1 samples. In contrast, a maximum conductivity was not reached for the ES-2 samples until after

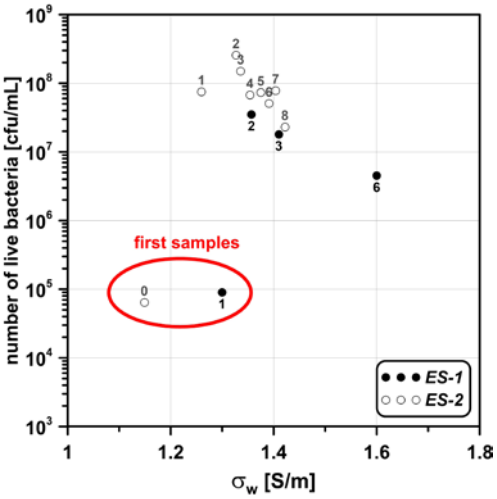

Figure 11: *Number of live bacteria in fluid vs fluid conductivity for the ES-1 and ES-2 samples. The shown data were all measured within the first 8 days. The numbers on the circles denote the day of harvest.*

8 days while the tests with the highest concentration of bacteria (ES-doub) reached the maximum after two days with a decrease thereafter. An explanation for this can be the seven phases of bacterial growth after Buchanan (1918) as described in Revil et al. (2012) where an exponential increase of bacterial growth can be found in phase 3 followed by the decreasing growth rate due to gradual decrease in substrate concentration in phase 4. In our experiment, the nutrients seem to be exhausted already after two days, and the bacteria might start to die which results in a bacterial decay. It is also conceivable that resulting toxic substances might poison cells (Mellage et al., 2019). That the changes can be linked to growth of cells is supported by similar observations from the plate counting, where only the live bacteria present in the fluid would be detected (Figure 8a), including a rapid decrease in the concentration of bacteria found associated with the ES-doub tests.

By comparing the number of live bacteria in the fluid (plate counting) with the conductivity of the filtered fluid for the first 8 days (Figure 11), two observations were made. First, the starting samples always showed low numbers of bacteria because they were still in the growing phase (Buchanan 1918). Second, both ES samples (ES-1 and ES-2) showed an increase in conductivity with a decreasing number of live bacteria after the first day. A possible explanation is that not only live bacteria have an influence on the fluid conductivity σw but also dead bacteria, likely via charges that can be carried by and their cellular by-products which are left in the fluid when the cells die and lyse. So, while the numbers of live bacteria decreased, the total cell mass in the experiment remained stable. One possible way to examine this in future experiments would be to use flow cytometry, where it is possible to quantify both live and dead cells in liquid (Prest et al., 2013).

Our results are not in full agreement with the results presented by Abdel Aal et al. (2010). They reported that, in sand column experiments, the low-frequency electrical measurements were sensitive to the presence of live bacterial cells and that the concentration of dead cells had only a minimal effect on both the real conductivity and imaginary conductivity. One possible explanation for the difference is that in Abdel Aal et al. (2010), SIP measurements were conducted directly on sand samples, while this study used filtered fluid separated from the sand. In addition, the bacteria examined by Abdel Aal and colleagues (2010) was Pseudomonas aeruginosa. While these bacteria have a highly similar cell structure to *E. coli*, they could differ in their surface and other properties. As detailed descriptions of how specific biological components influence conductivity are not available, it cannot be ruled out that the differences observed between these two studies are due to the differences in the type of bacteria that were examined. The surface of both of these Gram-negative bacteria is protected by a carbohydrate layer of lipopolysaccharide, which can influence hydrophobicity and biofilm characteristics, and which can vary widely between different species, and even different strains (or serotypes) of a single species (Ruhal et al., 2015). It would be interesting to examine, for example, purified lipopolysaccharide from different types of bacteria to assess molecular structural influences on conductivity.

The resistivities of the sand mixtures containing bacteria were predominantly lower compared to the mixtures without the presence of bacteria (media- or water-sand samples). These results are in accordance with the conductivities from the same fluid samples (σw). However, some outliers did occur. This may have been caused by possible small differences during packing of the sand in the sample holder, resulting in porosity differences and a higher formation factor. The presence of bacteria in the sand also impacted the phase. The media-sand and water-sand mixtures had almost no phase effect (+/- 0.5 mrad). Higher variation of phase values was detected for the bacteria-sand samples. A slightly increasing positive phase effect was seen for the ES-1 samples. Although no general clear tendency could be observed for all samples, a maximum at Day 6 for the ES-1 sample was seen which did not correlate with the maximum number of live bacteria (Figure 8a). Instead, the phase maximum correlated with the maximum in the fluid conductivity σw (Figure 3). At the same sample, two, albeit unidentified, small molecules were detected which suggest that the increasing phase may also have been influenced by the presence of these metabolites produced by the bacteria: bacteria consume and produce different molecules during growth, particularly if they are experiencing oxygen limitation (Clark, 1989). This is significant when considering measurements of bioremediation process using these methods since it may be beneficial to measure metabolism, and not just the presence or growth of bacteria.

In the beginning of the incubation of the bacteria-sand mixtures, small changes in the number of the inoculated bacteria (0.1% of the total mass) had a large impact on the resistivity of the samples. A doubling of the initial bacterial inoculation coincided with almost a halving of the initial resistivity (Figure 6a and c): at Day 0, the ES-2 sand sample with an inoculation amount of 0.15 mL bacteria showed a resistivity value of 13.2 Ωm (@ 1 Hz), while samples ES-doub with 0.3 mL bacteria inoculation had 6.3 Ωm at the same day and frequency. That holds also for Day 1 (ES-2: 8.9 Ωm, ES-doub: 4.7 Ωm). In contrast to the clear changes observed in conductivity and resistivity, the phase effects were very small (few mrad). This was expected and in accordance with results reported by other authors (e.g., Ntarlagiannis et al., 2005). Additionally, the small phase effects in the current study may have been influenced by the low concentrations of bacteria used for inoculation, and the influences from the salinity of the LB media. High fluid salinities decrease the phase response due to the masking by the bulk conductivity (Kruschwitz, 2008) so a lower salinity might have been preferred in order to observe higher phase effects.

Other studies have shown that by-products and the beginning formation of biofilm can increase the ionic conduction (Malvankar et al., 2012; Beyenal & Babauta 2015; Kessouri et al., 2019) as well as the imaginary conductivity (Davis et al., 2006). It is also known that "bioclogging", that is changes in the flow between areas due to biofilm formation, change the SIP response (Davis et al., 2006, 2010; Ntarlagiannis & Ferguson, 2009; Wu et al., 2014). Even though the aim of our study was to investigate the influence of bacteria on the SIP signal, and our results suggest these kinds of findings and support the conclusion of the other authors, only one isolated potential IP event was observed for the ES-1 Day 6 sample. The measured maximum phase signal for that samples was positive instead of the expected negative values which physically can be explained by inductive effects, by the sensitivity zone distribution in heterogeneous material (Wang et al., 2021) or, by occurring electrochemical changes within the samples.

But the positive phase signal could also be due to insufficient measurement accuracy due to a not optimized SIP setup, resulting in a random distribution of the phase values due to their small magnitudes. On the other hand, the observation that the significant different in the ES-1 phase values coincided with the detection of small, charged molecules that were only observed for that specific sample. In contrast to the resistivity resp. conductivity results, the polarization results are difficult to interpret, and conclusions can only be drawn cautiously. To overcome that problem the next time, an error analysis is needed resulting in an improve-

ment for the following experiments: As mentioned earlier, the salinity of the media was too high and unrealistic for field conditions. That needs to be reduced since the salinity decrease the IP effect. The sample holder construction was also not optimized for unconsolidated samples which probably affected the SIP measurements as well. For very high (> 1 kHz) and very low frequencies (< 10 mHz) some noise could be occasionally observed in the data. In contrast to many other studies which have used sand columns where fluid containing different cell densities passed through the sand (Abdel Aal et al., 2004, 2009; Ntarlagiannis et al., 2005; Davis et al., 2006; Mellage et al., 2018), this study first grew the bacteria as a biofilm on sand before being observed. As the majority of bacteria in nature prefer biofilm as a mode of growth, this experimental setup was chosen to offer a different set of conditions than examined in previous studies, while attempting to approximate the biofilm growth conditions encountered in nature. Unfortunately, our experimental design has caused difficulties since the sample packing and removal in and from the sample holder may have impacted the biofilm due to the physical movement of the sand. This would likely disturb biofilm connections between sand grains, although the biofilm growing on the surface of the grains would be intact. In addition, the packing was done manually which may have caused differences in the porosity which in turn affected the resistivity and phase results. A further error influencing factor could be the static condition of the sample compared to the active flow experiments by the other authors. That might have also caused bacterial changes, because no fresh nutrients could be provided, and no toxic by-products would be removed. Both issues can cause early death of the bacteria. In future experiments, quality control of the laboratory measurements needs to be improved. Even though we had the water-sand samples and the media-sand samples as control series and have done sample holder test measurements before with an experimental accuracy of +/- 0.2 mrad, further additional parallel samples, including additional laboratory SIP sample holders, would be helpful to rule out any erroneous measurements and strengthen conclusions.

5 Conclusions

The aim of this study was to find out how the presence of bacteria growing as biofilm can influence the SIP signal. Our findings showed that the fluid conductivity increased, and the resistivity decreased with increasing concentrations of bacteria and even small numbers of bacteria had a significant effect on the resistivity resp. the fluid conductivity. In phase, a lot of variations were found within a very small phase range, likely due to general small polarization effects and the high salinity of the LB media which masked the polarization effects. An increase of bacterial density generated a slight increase in phase; however, no significant trend could be observed possibly due to the not optimal experimental setup. The bacterial growth did not correlate with the maximum phase shift instead it could be attributed to the presence of two small, charged molecules that while unidentified, are likely specific metabolites of the *E. coli* strain used in the study. In general, the sensitivity of the SIP method should be able to resolve bacterial changes, but due to low phase effects, it would require different experimental design and high measurement accuracy to be applied in the field. More long-term experiments are needed, with improved and more extensive experimental design which also takes into account different nutrient media with lower salinity and mixes of different types of bacteria which naturally occur at contaminated sites. These experiments do suggest that geophysical methods are able to detect metabolic products from bacteria. This is significant since it supports the use of SIP for monitoring not the presence of bacteria in the subsurface, but instead their activities. This would be particularly useful for monitoring bioremediation in subsurface environments, where natural bacteria are numerous, and the goal is to observe stimulation of bacterial activity (which would result in production of metabolites) following different remediation interventions to remove unwanted chemical compounds. It remains to be seen if SIP would be able to distinguish between different metabolites or combinations that would be able to give high resolution information about specific bioremediation activities.

Acknowledgments, Samples, and Data

Lund University Bioimaging Centre (LBIC), Lund University, is gratefully acknowledged for analysis and discussions of the scanning electron microscopy images. Linda Jansson and Christer Larsson at Applied Microbiology, Lund University are thanked for their help and discussions regarding qPCR, and for conducting and contributing the HPLC analysis.

The experiments were funded by the MIRACHL project, funded by Formas, a Swedish government research council for sustainable development, (ref. 2016-20099 & 2016-00808), Geological Survey of Sweden and Lund University. This project has also received funding from the European Union's Horizon 2020 Research and Innovation Program under the Marie Sklodowska-Curie Grant agreement No. 752671.

References

Abdel Aal G.Z., Atekwana E.A., Slater L.D. & Atekwana E.A. (2004) Effects of microbial processes on electrolytic and interfacial electrical properties of unconsolidated sediments. Geophysical Research Letters, 31, L12505.

Abdel Aal G.Z., Atekwana E.A., Radzikowski S. & Rossbach S. (2009) Effect of bacterial adsorption on low frequency electrical properties of clean quartz sands and iron-oxide coated sands. Geophysical Research Letters, 36, L04403.

Abdel Aal G.Z., Atekwana E.A. & Atekwana E.A. (2010) Effect of bioclogging in porous media on complex conductivity signatures. Journal of Geophysical Research: Biogeosciences, 115, G00G07.

Albrecht R., Gourry J.C., Simonnot M.-O. & Leyval C. (2011) Complex conductivity response to microbial growth and biofilm formation on phenanthrene spiked medium. Journal of Applied Geophysics 75, 558–564.

Archer, C.T., Kim, J.F., Jeong, H., Park, J.H., Vickers, C.E., Lee, S.Y. and Nielsen, L.K., 2011. The genome sequence of *E. coli* W (ATCC 9637): comparative genome analysis and an improved genome-scale reconstruction of *E. coli*. BMC genomics, 12(1), pp.1-20.

Atekwana, E.A., Atekwana E.A., Werkema D.D., Allen J.P., Smart L.A., Duris J.W., Cassidy D.P., Sauck W.A. & Rossbach S., (2004a): Evidence for microbial enhanced electrical conductivity in hydrocarbon contaminated sediments. Geophysical Research Letters, 31. 1-4.

Atekwana E.A., Werkema D.D., Duris J.W., Rossbach S., Atekwana E.A., Sauck W.A., et al. (2004b) In-situ apparent conductivity measurements and microbial population distribution at a hydrocarbon-contaminated site. Geophysics, 69, 56– 63.

Atekwana E.A. & Slater L.D. (2009) Biogeophysics: a new frontier in earth science research. Reviews of Geophysics, 47, RG4004.

Atekwana E.A. & Atekwana E.A. (2010) Geophysical signatures of microbial activity at hydrocarbon contaminated sites: a review. Surveys in Geophysics, 31, 247–283.

Auken, E., J. Doetsch, G. Fiandaca, A. Vest Christiansen, A. Gazoty, A.G. Cahill, & Jakobsen, R. (2014) Imaging subsurface migration of dissolved CO2 in a shallow aquifer using 3-D time-lapse electrical resistivity tomography. Journal of Applied Geophysics, 101, 31–41. https://doi.org/10.1016/j.jappgeo.2013.11.011

Berg, J.M., Tymoczko, J.L. & Styer, L., (2006) Biochemistry, 6th Edition. W.H. Freeman and Company, New York. 1021 pp.

Beyenal H. & Babauta J.T. (2015) Biofilms in Bioelectrochemical Systems: From Laboratory Practice to Data Interpretation. Hoboken, NJ: John Wiley & Sons.

Binely, A. & Slater, L. (2020) Resistivity and Induced Polarization: Theory and Applications to the Near-Surface Earth. Cambridge University Press

Branda, S.S., Vik, S., Friedman, L. & Kolter, R. (2005) Biofilms: the matrix revisited. Trends in Microbiology, 13(1), 20-6. doi: 10.1016/j.tim.2004.11.006.

Brovelli, A., Malaguerra, F. & Barry, D., (2009) Bioclogging in porous media: Model de-velopment and sensitivity to initial conditions. Environmental Modelling & Software, 24, 611-626.

Buchanan, R. E. (1918) Life phases in a bacterial culture, J. Infect. Dis., 23, 109–125.

Burri, N.M., Weatherl, R., Moeck, C. & Schirmer, M. (2019) A review of threats to groundwater quality in the anthropocene. Science of the total environment, 684, 136-154.

Cardarelli, E., & Di Filippo, G. (2009) Electrical resistivity and induced polarization tomography in identifying the plume of chlorinated hydrocarbons in sedimentary formation: a case study in Rho (Milan – Italy). Waste Management & Research, 27: 595-602. doi: 10.1177/0734242X09102524

Clark, D.P. (1989) The fermentation pathways of *Escherichia coli*. FEMS microbiology reviews, 5(3), pp.223-234.

Davis C.A., Atekwana E.A., Atekwana E.A., Slater L.D., Rossbach S. & Mormile M.R. (2006) Microbial growth and biofilm formation in geologic media is detected with complex conductivity measurements. Geophysical Research Letters, 33, L18 403.

Davis C.A., Pyrak-Nolte L.J., Atekwana E.A., Werkema D.D. & Haugen M.E. (2010) Acoustic and electrical property changes due to microbial growth and biofilm formation in porous media. Journal of Geophysical Research: Biogeosciences 115, 1–14.

EEA (European Environment Agency), (2019) The European environment — state and outlook 2020. Catalogue Number: TH-04-19-541-EN-N, doi:10.2800/96749

Elbing, K.L. & Brent, R., 2019. Recipes and tools for culture of *Escherichia coli*. Current protocols in molecular biology, 125(1), p.e83.

Erdoğan, S.T., Forster, A.M., Stutzman, P.E. & Garboczi, E.J. (2017) Particle-based characterization of Ottawa sand: Shape, size, mineralogy, and elastic moduli. Cement and Concrete Composites, 83, 36-44, https://doi.org/10.1016/j.cemconcomp.2017.07.003.

Flores Orozco, A., Williams, K.H., Long, P.E., Hubbard, S.S. & Kemna, A. (2011) Using complex resistivity imaging to

infer biogeochemical processes associated with bioremediation of an uranium-contaminated aquifer. Journal of Geophysical Research, 116 (G3), G03001.

Flores Orozco, A., Kemna, A., Oberdörster, C., Zschornack, L., Leven, C., Dietrich, P. & Weiss, H. (2012) Delineation of subsurface hydrocarbon contamination at a former hydrogenation plant using spectral induced polarization imaging. Journal of Contaminant Hydrology, 136-137, 131–144.

Imlay, J.A., (2013) The molecular mechanisms and physiological consequences of oxidative stress: lessons from a model bacterium. Nature Reviews Microbiology, 11(7), pp.443-454.

Johansson, S., Fiandaca, F. & Dahlin, F. (2015) Influence of non-aqueous phase liquid configuration on induced polarization parameters: Conceptual models applied to a time-domain field case study. Journal of Applied Geophysics, 123: 295-309. http://dx.doi.org/10.1016/j.jappgeo.2015.08.010

Kessouri, P., Furman, A., Huisman, J., Martin, T., Mellage, A., Ntarlagiannis, D., Bücker, M. et al. (2019), Induced polarization applied to biogeophysics: recent advances and future prospects. Near Surface Geophysics, 17: 595-621. doi:10.1002/nsg.12072

Kruschwitz, S. (2008), Assessment of the complex resistivity behavior of salt affected building materials, PhD thesis, TU Berlin, Germany.

Malvankar N.S., Mester T., Tuominen M.T. & Lovley D.R. (2012) Supercapacitors based on c-type cytochromes using conductive nanostructured networks of living bacteria. ChemPhysChem, 13, 463–468.

Mellage A., Smeaton C.M., Furman A., Atekwana E.A., Rezanezhad F. & Van Cappellen P. (2018) Linking spectral induced polarization (SIP) and subsurface microbial processes: results from sand column incubation experiments. Environmental Science and Technology, 52, 2081–2090.

Mellage A., Smeaton C.M., Furman A., Atekwana E.A., Rezanezhad F. & Van Cappellen P. (2019) Bacterial Stern layer diffusion: experimental determination with spectral induced polarization and sensitivity to nitrite toxicity. Near Surface Geophysics, 17, 623-635

Nadkarni, M.A., Martin, F.E., Jacques, N.A. & Hunter, N. (2002) Determination of bacterial load by real-time PCR using a broad-range (universal) probe and primers set. Microbiology 148: 257-266.

Nivorlis, A., Dahlin, T., Rossi, M., Höglund, N. & Sparrenbom, C. (2019) Multidisciplinary characterization of chlorinated solvents contamination and in-situ remediation with the use of the Direct Current resistivity and time-domain Induced Polarization tomography. Geosciences, 9, 1-16. https://doi.org/10.3390/geosciences9120487

Ntarlagiannis, D., Yee, N. & Slater, L. (2005) On the low-frequency electrical polarization of bacterial cells in sands. Geophysical Research Letter, 32, L24402, doi:10.1029/2005GL024751

Ntarlagiannis D. & Ferguson, A. (2009) SIP response of artificial biofilms. Geophysics, 74, A1–A5.

Ontash & Ermac, (2018) O & E portable spectral induced polarization (SIP) field/lab unit (PSIP) user guide. Ontash & Ermac, Inc, http://www.ontash.com

Osborne, M.G., Geiger, C.J., Corzett, C.H., Kram, K.E. & Finkel, S.E., (2021) Removal of Toxic Volatile Compounds in Batch Culture Prolongs Stationary Phase and Delays Death of *Escherichia coli*. Applied and Environmental Microbiolo-gy, 87(24), pp.e01860-21.

Power, C., Gerhard, J.I., Karaoulis, M., Tsourlos, P. & Giannopoulos, A. (2014) Evaluating fourdimensional time-lapse electrical resistivity tomography for monitoring DNAPL source zone remediation. Journal of Contaminant Hydrology 162: 27–46.

Prest, E.I., Hammes, F., Kötzsch, S., Van Loosdrecht, M.C.M. & Vrouwenvelder, J.S., (2013) Monitoring microbiological changes in drinking water systems using a fast and reproducible flow cytometric method. Water research, 47(19), pp.7131- 7142.

Prodan C., Mayo F., Claycomb J., Miller Jr J. & Benedik M. (2004) Low-frequency, low-field dielectric spectroscopy of living cell suspensions. Journal of Applied Physics, 95, 3754–3756.

Revil, A., Atelwana, E., Zhang, C., Jardani, A. & Smith, S. (2012) A new model for the spectral induced polarization signature of bacterial growth in porous media. Water Resources Research, 48, W09545, doi:10.1029/2012WR011965

Rochex, A., Godon, J.J., Bernet, N. and Escudié, R., 2008. Role of shear stress on composition, diversity and dynamics of biofilm bacterial communities. Water Research, 42(20), pp.4915-4922.

Rodrigues, S.M. & Römkens, P.F. (2018) Human health risks and soil pollution. Soil Pollution, 217-250. Academic Press.

Rosier, C.L., Atekwana, E.A., Abdel Aal, G. & Patrauchan, M.A. (2019) Cell concentrations and metabolites enhance the SIP response to biofilm matrix components. Journal of Applied Geophysics, 160, 183-194

Rosqvist, H., Leroux, V., Dahlin, T., Svensson, M., Lindsjö, M., Månsson, C-H. & Johansson, S. (2011) Mapping landfill gas migration using resistivity monitoring. Waste Resour. Manag., 164, 3–15.

Ruhal, R., Antti, H., Rzhepishevska, O., Boulanger, N., Barbero, D.R., Wai, S.N., Uhlin, B.E. & Ramstedt, M. (2015) A multivariate approach to correlate bacterial surface properties to biofilm formation by lipopolysaccharide mutants of Pseudomonas aeruginosa. Colloids and Surfaces B: Biointerfaces, 127, pp.182-191.

Saneiyan S., Ntarlagiannis D., Dale Werkema Jr., D. & Ustra, A. (2018) Geophysical methods for monitoring soil stabilization processes. Journal of Applied Geophysics, 148, 234 – 244.

Sparrenbom, C.J., Akesson, S., Johansson, S., Hagerberg, D. & Dahlin, T. (2017) Investigation of chlorinated solvent pollution with resistivity and induced polarization. Science of the Total Environment, 575, 767-778.

Stroo, H.F., Leeson, A. & Ward, C.H. (eds.) (2013) Bioaugmentation for Groundwater Remediation. New York: Springer. 389 pp.

Voroney, R.P. (2007) The Soil Habitat. Paul, E.A (Ed.) Soil Microbiology, Ecology and Biochemistry (3rd Edition), Academic Press, pp. 552 (25-49)

Wang, C., Binley, A. & Slater, L.D., (2021) On negative induced polarization in frequency domain measurements, Geophysical Journal International, 225 (1), 342–353, https://doi.org/10.1093/gji/ggaa581

Waxman, M.H. & Smits, L.J.M. (1968) Electrical Conductivities in Oil-Bearing Shaly Sands. Society of Petroleum Engineers Journal, 8, 107-122. http://dx.doi.org/10.2118/1863-A